

# HADRON STRUCTURES AND PERTURBATIVE QCD <sup>a</sup>

YUJI KOIKE

*Department of Physics, Niigata University  
Ikarashi, Niigata 950-2181, Japan  
E-mail: koike@nt.sc.niigata-u.ac.jp*

In the first part of this talk, I will summarize recent developments in the study of the chiral-odd spin-dependent parton distributions  $h_1(x, Q^2)$  and  $h_L(x, Q^2)$  of the nucleon, in particular, (i) Next-to-leading order  $Q^2$  evolution of  $h_1(x, Q^2)$  and (ii) Leading order  $Q^2$  evolution of the twist-3 distribution  $h_L(x, Q^2)$  and the universal simplification of the  $Q^2$  evolution of all the twist-3 distributions in the large  $N_c$  limit. The second part of this talk will be devoted to a systematic analysis on the light-cone distribution amplitudes of vector mesons ( $\rho$ ,  $\omega$ ,  $\phi$ ,  $K^*$  etc) relevant for exclusive processes producing these mesons. In particular, twist-3 distribution amplitudes are discussed in detail.

## 1 Introduction

High energy processes can be classified into two categories, inclusive and exclusive processes. Quark-gluon substructures of hadrons involved in these processes reveal themselves as a form of parton distribution functions in the inclusive processes, and light-cone distribution amplitudes in the exclusive processes. Understanding on both quantities constitutes a crucial step for the QCD description of the high energy processes. In this talk, I will summarize our recent studies on the quark distribution functions in the nucleon and the light-cone distribution amplitudes for the light vector mesons.

Spin dependent parton distribution functions for the nucleon measured by the polarized beams and targets represent “spin distributions” carried by quarks and gluons inside the nucleon. They are functions of Bjorken’s  $x$  which represent parton’s momentum fraction in the nucleon and a scale  $Q^2$  at which they are measured. Until now, most data on the nucleon’s distribution functions have been obtained through the lepton-nucleon deep inelastic scattering (DIS). The chiral-odd distributions,  $h_{1,L}(x, Q^2)$ , are the new type of distribution functions which have not been measured so far: Due to the chiral-odd nature, they decouple from the inclusive DIS. They can, however, be measured by the nucleon-nucleon polarized Drell-Yan process and semi-inclusive DIS which detect particular hadrons in the final state. They will hopefully be measured by planned experiments using polarized accelerators at BNL, DESY, CERN and SLAC etc<sup>1</sup>. In particular, RHIC at BNL is expected to provide first data on these distributions.

In the study of these distribution functions, perturbative QCD plays an important role in predicting their  $Q^2$ -dependence: Given a distribution function, say  $h_1(x, Q_0^2)$ , at one scale  $Q_0^2$ , perturbative QCD predicts the shape of  $h_1(x, Q^2)$  at an arbitrary scale  $Q^2$ . This  $Q^2$  evolution is necessary not only in extracting low energy hadron properties from high energy experimental data but also in testing the  $x$ -dependence predicted by a non-perturbative QCD technique or a model with the high energy data. In the first part of this talk, I will summarize our recent studies on the  $Q^2$ -dependence of  $h_{1,L}(x, Q^2)$ .

Light-cone distribution amplitudes (wave functions) for the vector mesons ( $\rho, \omega, \phi$ , and  $K^*$ ) appear in various exclusive processes producing these vector mesons in final states, such as  $B$  decay,  $B \rightarrow \ell \nu V$ ,  $B \rightarrow \ell^+ \ell^- V$ ,  $B \rightarrow \gamma V$ , and electro-production,  $e + N \rightarrow N' + V$ . (Study on the wave functions for pseudoscalar mesons is less involved, and has been done by many works.) Analysis on the wave functions is indispensable to test applicability of perturbative QCD to exclusive processes. In particular, test of the standard model through the rare  $B$  decay requires the knowledge on these wave functions. In the second part of this talk, we present a complete classification of the two-particle (quark-antiquark) wave functions for the vector mesons based on twist, chirality and spin. This can be done in parallel with that for the nucleon’s parton distribution functions. In particular, for the

---

<sup>a</sup>Invited talk presented at “RCNP International School of Physics of Hadrons and QCD”, October 12-13, 1998, Osaka, Japan. To be published in the proceedings.

twist-3 wave functions, we identify the contribution from the three-particle (quark-gluon-antiquark) twist-3 distribution amplitudes, using QCD equation of motion. The renormalization and the model building for the twist-3 wave functions can be/should be done starting from these exact relations, which is discussed by Tanaka in the workshop.

## 2 Distribution Function of the Nucleon in Inclusive Processes

### 2.1 Chiral-Odd Distributions $h_{1,L}(x, Q^2)$

Inclusive hard processes can be generally analyzed in the framework of the QCD factorization theorem<sup>2</sup>. This theorem generalizes the idea of the Bjorken-Feynman's "parton model" and allows us to include QCD correction in a systematic way. Here I restrict myself to the hard processes with the nucleon target, such as deep-inelastic lepton-nucleon scattering (DIS,  $l + p \rightarrow l' + X$ ), Drell-Yan ( $p + p' \rightarrow l^+ l^- + X$ ), semi-inclusive DIS ( $l + p \rightarrow l' + h + X$ ). According to the above theorem, the cross section (or the nucleon structure function) for these processes can be factorized into a "soft part" and a "hard part": The soft part represents the parton (quark or gluon) distribution in the nucleon and the hard part describes the short distance cross section between the parton and the external hard probe which is calculable within perturbation theory. For example, a nucleon structure function in DIS can be written as the imaginary part of the virtual photon-nucleon forward Compton scattering amplitude. (Fig. 1 (b)) According to the above theorem, in the Bjorken limit, i.e.  $Q^2, \nu = P \cdot q \rightarrow \infty$  with  $x = Q^2/2\nu = \text{finite}$ , ( $Q^2 = -q^2$  is the virtuality of the space-like photon,  $P$  is the nucleon's four momentum), the structure function can be written as

$$W(x, Q^2) = \sum_a \int_x^1 \frac{dy}{y} H^a\left(\frac{x}{y}, \frac{Q^2}{\mu^2}, \alpha_s(\mu^2)\right) \Phi^a(y, \mu^2), \quad (1)$$

where  $\Phi^a$  represents a distribution of parton  $a$  in the nucleon and  $H^a$  describes the short distance cross section of the parton  $a$  with the virtual photon.  $\mu^2$  is the factorization scale. In Fig. 1(b),  $\Phi^a$  is identified by the dotted line. (Fig.1 (a)). Similarly to DIS, the cross section for the nucleon-nucleon Drell-Yan process can also be written in a factorized form at  $s = (P_A + P_B)^2$ ,  $Q^2 \rightarrow \infty$  with a fixed  $Q^2/s$  ( $P_{A,B}$  are the momenta of the two nucleons,  $Q$  is the momentum of the virtual photon):

$$d\sigma \sim \sum_{a,b} \int_{x_a}^1 dy_a \int_{x_b}^1 dy_b H^{ab}\left(\frac{x_a}{y_a}, \frac{x_b}{y_b}, Q^2; \frac{Q^2}{\mu^2}, \alpha_s(\mu^2)\right) \Phi^a(y_a, \mu^2) \Phi^b(y_b, \mu^2), \quad (2)$$

where the two parton distributions,  $\Phi^a$  and  $\Phi^b$ , for the beam and the target appear as was shown by dotted lines in Fig. 1(c).

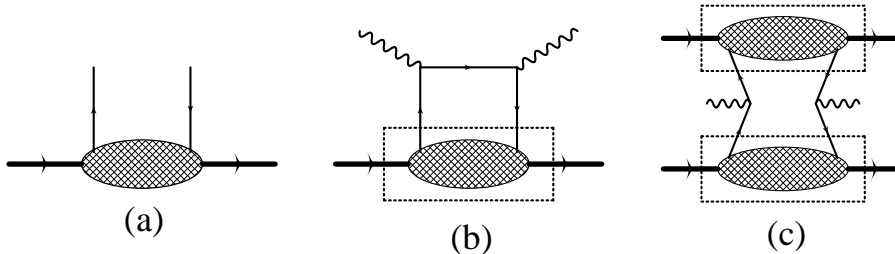


Figure 1: (a) Quark distribution function. (b) Nucleon structure function in DIS. (c) Cross section for the nucleon-nucleon Drell-Yan process.

As is seen from Figs. 1(b),(c), the parton distribution can be regarded as a parton-nucleon forward scattering amplitude shown in Fig. 1 (a) which appear in several different hard processes.

In particular, the quark distribution in the nucleon moving in the  $+\hat{e}_3$  direction can be written as the light-cone Fourier transform of the quark correlation function in the nucleon:<sup>3</sup>

$$\Phi^a(x, \mu^2) = P^+ \int_{-\infty}^{\infty} \frac{dz^-}{2\pi} e^{ixP \cdot z} \langle PS | \bar{\psi}^a(0) \Gamma \psi^a(z) |_{\mu} | PS \rangle, \quad (3)$$

where  $|PS\rangle$  denotes the nucleon (mass  $M$ ) state with momentum  $P^\mu$  and spin  $S^\mu$ , and  $\psi^a$  is the quark field with flavor  $a$ . In (3), we have suppressed for simplicity the gauge link operator which ensures the gauge invariance and  $|_{\mu}$  indicates the operator is renormalized at the scale  $\mu^2$ . A four vector  $a^\mu$  is decomposed into two light-cone components  $a^\pm = \frac{1}{\sqrt{2}}(a^0 \pm a^3)$  and the transverse component  $\vec{a}_\perp$ . In (3),  $z^+ = 0$ ,  $\vec{z}_\perp = \vec{0}$ , and  $z^2 = 0$ .  $\Gamma$  generically represents  $\gamma$ -matrices,  $\Gamma = \gamma_\mu, \gamma_\mu \gamma_5, \sigma_{\mu\nu}, 1$ .  $\Phi^a(x, \mu^2)$  measures the distribution of the parton  $a$  to carry the momentum  $k^+ = xP^+$  in the nucleon, which is independent from particular hard processes.

If one puts  $\Gamma = \gamma_\mu, \gamma_\mu \gamma_5$ , the chirality of  $\bar{\psi}$  and  $\psi$  becomes the same, namely it defines the chiral-even distributions. Likewise, putting  $\Gamma = \sigma_{\mu\nu}, 1$  defines the chiral-odd distributions. For the case of the deep-inelastic scattering (Fig. 1 (b)), the quark line emanating from the target nucleon comes back to the original nucleon after passing through the hard interactions. Since the perturbative interaction in the standard model preserves the chirality except a tiny quark mass effect, the chirality of the two quark lines entering the nucleon in Fig. 1(b) is the same. Hence the DIS can probe only the chiral-even quark distributions. On the other hand, in the Drell-Yan process (Fig. 1 (c)), there is no correlation in chirality between two quark lines entering each nucleon. Therefore the Drell-Yan process probes both chiral even and odd distributions.

The chiral-odd distributions  $h_1^a(x, \mu^2)$ ,  $h_L^a(x, \mu^2)$  in our interest are defined by putting  $\Gamma = \sigma_{\mu\nu} i \gamma_5$  in (3):<sup>4</sup>

$$\begin{aligned} & \int \frac{d\lambda}{2\pi} e^{i\lambda x} \langle PS | \bar{\psi}^a(0) \sigma_{\mu\nu} i \gamma_5 \psi^a(\lambda n) |_{\mu} | PS \rangle \\ &= 2[h_1^a(x, \mu^2)(S_{\perp\mu} p_\nu - S_{\perp\nu} p_\mu)/M \\ &+ h_L^a(x, \mu^2)M(p_\mu n_\nu - p_\nu n_\mu)(S \cdot n) \\ &+ h_3^a(x, \mu^2)M(S_{\perp\mu} n_\nu - S_{\perp\nu} n_\mu)] \end{aligned} \quad (4)$$

where we introduced two light-like vectors  $p, n$  ( $p^2 = n^2 = 0$ ) by the relation  $P^\mu = p^\mu + \frac{M^2}{2}n^\mu$ ,  $p \cdot n = 1$ ,  $p^- = n^+ = 0$ . If we write  $P^+ = \mathcal{P}$ ,  $p = \frac{\mathcal{P}}{\sqrt{2}}(1, 0, 0, 1)$ ,  $n = \frac{1}{\sqrt{2}\mathcal{P}}(1, 0, 0, -1)$ .  $\mathcal{P}$  is a parameter which specifies the Lorentz frame of the system:  $\mathcal{P} \rightarrow \infty$  corresponds to the infinite momentum frame, and  $\mathcal{P} \rightarrow M/\sqrt{2}$  the rest frame of the nucleon.  $S_\perp^\mu$  is the transverse component of  $S^\mu$  defined by  $S^\mu = (S \cdot n)p^\mu + (S \cdot p)n^\mu + S_\perp^\mu$ . One can show that  $\Phi^a$  defined in (3) has a support  $-1 < x < 1$ . If one replaces the quark field  $\psi$  in (3) by its charge conjugation field  $C\bar{\psi}^T$ , it defines the anti-quark distribution  $\bar{\Phi}^a$ . In particular  $h_{1,L,3}^a(x, \mu^2)$  in (4) are related to their anti-quark distribution by  $h_{1,L,3}^a(-x, \mu^2) = -\bar{h}_{1,L,3}^a(x, \mu^2)$ .

$\Phi^a$  appears in a physical cross section in the form of the convolution with a short distance cross section in a parton level as is shown in (1) and (2). The cross section can be expanded in powers of  $\frac{1}{\sqrt{Q^2}}$  as

$$\sigma(Q^2) \sim A(\ln Q^2) + \frac{M}{\sqrt{Q^2}} B(\ln Q^2) + \frac{M^2}{Q^2} C(\ln Q^2) + \dots, \quad (5)$$

where each coefficient  $A, B, C$  receives logarithmic  $Q^2$ -dependence due to the QCD radiative correction. In order to see how  $h_{1,L,3}$  can contribute in the expansion (5), it is convenient to move into the infinite momentum frame ( $\mathcal{P} \sim Q \rightarrow \infty$ ). In this limit the coefficient of  $h_{1,L,3}$  in (4) behaves, respectively, as  $O(Q), O(1), O(1/Q)$ . Therefore if  $h_1$  contributes to the  $A$  term in (5),  $h_L$

spin	average	longitudinal	transverse
twist-2	$f_1$	$g_1$	$\underline{h_1}$
twist-3	$\underline{e}$	$\underline{h_L}$	$g_T$

Table 1: Classification of the quark distributions based on spin, twist and chirality. Underlined distributions are chiral-odd. Others are chiral-even.

can contribute at most to the  $B$ -term, and  $h_3$  can contribute at most to the  $C$ -term. In general, when a distribution function contributes to hard processes at most in the order of  $\left(\frac{1}{\sqrt{Q^2}}\right)^{\tau-2}$ , the distribution is called twist- $\tau$ . Therefore  $h_1$ ,  $h_L$ ,  $h_3$  in (4) is, respectively, twist-2, -3 and -4.

Twist-2 distribution  $h_1$  can be measured through the transversely polarized Drell-Yan<sup>5,6,4,7</sup>, semi-inclusive deep inelastic scatterings which detect pion<sup>8</sup>, polarized baryons<sup>6,9,10</sup>, correlated two pions<sup>11</sup>.

From the discussion above, one sees that it is generally difficult to isolate experimentally higher twist ( $\tau \geq 3$ ) distributions in hard processes, since they are hidden by the leading twist-2 contribution ( $A$  term in (5)). However, this is not the case for  $h_L$  and  $g_T$ . In particular spin asymmetries, they contribute to the  $B$ -term in the absence of  $A$ -term:  $g_T$  can be measured in the transversely polarized DIS<sup>12</sup>, and  $h_L$  appears in the longitudinal versus transverse spin asymmetry in the polarized nucleon-nucleon Drell-Yan process<sup>4</sup>. Therefore the  $Q^2$ -evolution of  $g_T$  and  $h_L$  can be a new test of perturbative QCD beyond the twist-2 level.

Insertion of other  $\gamma$ -matrices in (3) defines other distributions. In Table 1, we show the classification of the quark distributions up to twist-3<sup>4</sup>. There  $f_1$ ,  $g_{1,T}$ ,  $e$  is defined, respectively, by  $\Gamma = \gamma_\mu, \gamma_\mu \gamma_5, 1$  in (3). A similar classification can also be extended to the gluon distributions<sup>14</sup>. The distribution  $f_1$  contributes to the spin averaged structure functions  $F_{1,2}(x, Q^2)$  familiar in DIS. The helicity distribution  $g_1$  contributes to the  $G_1(x, Q^2)$  structure function measured in the longitudinally polarized DIS. By now there has been much accumulation of experimental data on  $f_1$  and  $g_1$ , and the data on  $g_1$  triggered lots of theoretical discussion on the ‘‘origin of the nucleon spin’’<sup>1</sup>. The first nonzero data on  $g_2$  ( $= g_T - g_1$ ) was also reported in Ref.<sup>13</sup>.

## 2.2 Next-to-leading order (NLO) $Q^2$ -evolution of $h_1(x, Q^2)$

As we saw in the previous section,  $h_1$  is the third and the final twist-2 quark distribution. It has a simple parton model interpretation as can be seen by the Fourier expansion of  $\psi$  in (4). It measures the probability in the transversely polarized nucleon to find a quark polarized parallel to the nucleon spin minus the probability to find it oppositely polarized. Here the transverse polarization refers to the eigenstate of the transverse Pauli-Lubański operator  $\gamma_5 \not{S}_\perp$ . If one replaces the transverse polarization by the longitudinal one, it becomes the helicity distribution  $g_1$ . For nonrelativistic quarks,  $h_1(x, \mu^2) = g_1(x, \mu^2)$ . A model calculation suggests,  $h_1$  is the same order as  $g_1$ .<sup>4,15,16</sup>

The  $Q^2$ -evolution of  $h_1$  is described by the usual DGLAP evolution equation<sup>17</sup>. Because of its chiral-odd nature it does not mix with gluon distributions. Therefore the  $Q^2$ -dependence of  $h_1$  is described by the same equation both for singlet and nonsinglet distributions. For  $f_1$  and  $g_1$ , the NLO  $Q^2$  evolution was derived long time ago<sup>18,19,20,21</sup> and has been frequently used for the analysis of experiments<sup>22,23</sup>. The leading order (LO)  $Q^2$ -evolution for  $h_1$  has been known for some time<sup>6</sup>. In the recent literature, the next-to-leading order (NLO)  $Q^2$ -evolution has also been completed by two papers<sup>24,25</sup>: Vogelsang<sup>24</sup> presented the light-cone gauge calculation for the two-loop splitting function of  $h_1$  in the formalism originally used for  $f_1$ <sup>20</sup>. We<sup>25</sup> carried out the Feynman gauge calculation of the two-loop anomalous dimension following the method of Ref.<sup>18</sup> for  $f_1$ . The results of these calculations in the  $\overline{\text{MS}}$  scheme agreed completely. In the following, I briefly discuss the characteristic feature of the NLO  $Q^2$  evolution of  $h_1$  following Refs.<sup>25,26</sup>.

Analysis of (4) gives the connection between the  $n$ -th moment of  $h_1$  and a tower of twist-2

operators:

$$\begin{aligned}\mathcal{M}_n[h_1(\mu^2)] &\equiv \int_{-1}^1 dx x^n h_1(x, \mu^2) = \frac{-1}{2M} \langle PS_\perp | O_n^\perp(\mu^2) | PS_\perp \rangle, \\ O_n^\perp &= S_{\perp\nu} \bar{\psi} \sigma^{\nu\alpha} n_\alpha i \gamma_5 (i n \cdot D)^n \psi,\end{aligned}\tag{6}$$

where  $S_\perp$  stands for the transverse polarization and  $O_n^\perp(\mu^2)$  indicates the operator  $O_n^\perp$  is renormalized at the scale  $\mu^2$ . The contraction with  $n^\mu$  and  $S_\perp^\mu$  (recall  $S_\perp \cdot n = 0$ ,  $n^2 = 0$ ) in (6) projects out the relevant twist-2 contribution from the composite operator. (“Twist” for local composite operators is defined as dimension minus spin.) By solving the renormalization group equation for  $O_n^\perp$ , one gets the NLO  $Q^2$  dependence of  $\mathcal{M}_n[h_1(\mu^2)]$  as

$$\frac{\mathcal{M}_n[h_1(Q^2)]}{\mathcal{M}_n[h_1(\mu^2)]} = \left( \frac{\alpha_s(Q^2)}{\alpha_s(\mu^2)} \right)^{\gamma_n^{(0)}/2\beta_0} \left[ 1 + \frac{\alpha_s(Q^2) - \alpha_s(\mu^2)}{4\pi} \frac{\beta_1}{\beta_0} \left( \frac{\gamma_n^{(1)}}{2\beta_1} - \frac{\gamma_n^{(0)}}{2\beta_0} \right) \right],\tag{7}$$

where  $\alpha_s(Q^2)$  is the NLO QCD running coupling constant given by

$$\frac{\alpha_s(Q^2)}{4\pi} = \frac{1}{\beta_0 \ln(Q^2/\Lambda^2)} \left[ 1 - \frac{\beta_1 \ln \ln(Q^2/\Lambda^2)}{\beta_0^2 \ln(Q^2/\Lambda^2)} \right],\tag{8}$$

with the one-loop and two-loop coefficients of the  $\beta$ -function  $\beta_0 = 11 - 2/3 N_f$  and  $\beta_1 = 102 - 38/3 N_f$  ( $N_f$  is the number of quark flavor) and the QCD scale parameter  $\Lambda$ .  $\gamma_n^{(0)}$  and  $\gamma_n^{(1)}$  are the one-loop and two-loop coefficients of the anomalous dimension  $\gamma_n$  for  $O_n^\nu S_{\perp\nu}$  defined as

$$\gamma_n = \frac{\alpha_s}{4\pi} \gamma_n^{(0)} + \left( \frac{\alpha_s}{4\pi} \right)^2 \gamma_n^{(1)}.\tag{9}$$

If one sets  $\beta_1 \rightarrow 0$  and  $\gamma_n^{(1)} \rightarrow 0$  in (7), the leading order (LO)  $Q^2$  evolution is obtained.  $\gamma_n^{(0)}$  and  $\gamma_n^{(1)}$  are obtained, respectively, by calculating the one-loop and two-loop corrections to the two-point Green function which imbeds  $O_n^\nu S_{\perp\nu}$ . To obtain  $\gamma_n^{(1)}$ , calculation of 18 two-loop diagrams is required in the Feynman gauge. Since the expression for  $\gamma_n^{(1)}$  is quite complicated, we refer the readers to Refs. <sup>24,25</sup> for them.

In order to get a rough idea about the NLO  $Q^2$  dependence of  $h_1$ , we plotted in Fig. 2  $\gamma_n^{h(1)}$  ( $\gamma_n^{(1)}$  for  $h_1$ ) in comparison with  $\gamma_n^{fg(1)}$  ( $\gamma_n^{(1)}$  for the nonsinglet  $f_1$  and  $g_1$ ) for  $N_f = 3, 5$ . One sees from Fig. 2  $\gamma_n^{h(1)} > \gamma_n^{fg(1)}$  especially at small  $n$ . This suggests that the NLO  $Q^2$  evolution of  $h_1$  is quite different from that of  $f_1$  and  $g_1$  in the small  $x$  region. The relation  $\gamma_n^{h(1)} > \gamma_n^{fg(1)}$  is in parallel with and even more conspicuous than the LO anomalous dimensions which read

$$\begin{aligned}\gamma_n^{h(0)} &= 2C_F \left( 1 + 4 \sum_{j=2}^{n+1} \frac{1}{j} \right), \\ \gamma_n^{fg(0)} &= 2C_F \left( 1 - \frac{2}{(n+1)(n+2)} + 4 \sum_{j=2}^{n+1} \frac{1}{j} \right).\end{aligned}\tag{10}$$

To illustrate the generic feature of the  $Q^2$  evolution, we have applied the obtained  $Q^2$  evolution to a reference distribution for  $g_1$  and  $h_1$ . As a reference distribution, we take GRSV  $g_1$  distribution<sup>23</sup> and assume  $h_1(x, \mu^2) = g_1(x, \mu^2)$  at a low energy input scale ( $\mu^2 = 0.23 \text{ GeV}^2$  for LO and  $\mu^2 = 0.34 \text{ GeV}^2$  for NLO evolution) as is suggested by a nucleon model<sup>4,15</sup>. We then evolve them to  $Q^2 = 20 \text{ GeV}^2$  and see how much deviation is produced between them. The result is shown in Fig. 3. As is

expected from the anomalous dimension, the drastic difference in the  $Q^2$  evolution between  $h_1$  and  $g_1$  is observed in the small  $x$  region, and this tendency is more significant for the NLO evolution.<sup>27,28,26</sup> (Although  $g_1$  for  $u$ -quark mixes with the gluon distribution, the same tendency in the difference from  $h_1$  is observed for the nonsinglet distribution.)

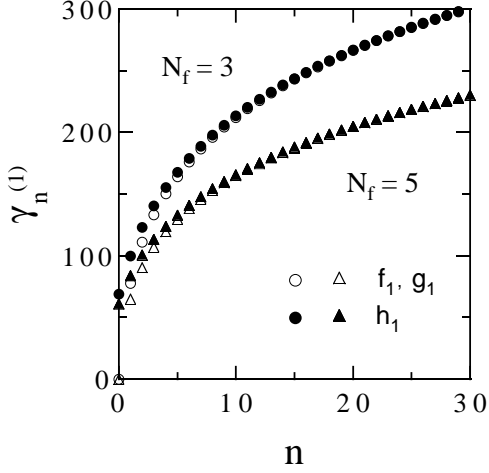


Figure 2: The NLO anomalous dimension  $\gamma_n^{h(1)}$  in comparison with  $\gamma_n^{fg(1)}$ . This figure is taken from Ref. <sup>25</sup>.

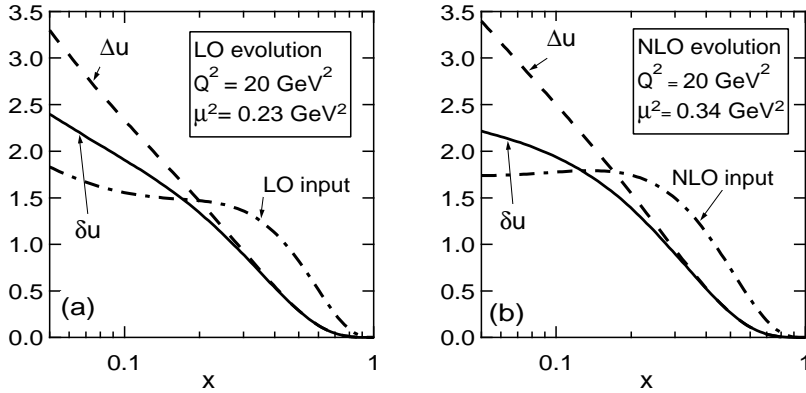


Figure 3: (a) The LO  $Q^2$  evolution of  $h_1$  (denoted by  $\delta u$ ) and  $g_1$  (denoted by  $\Delta u$ ) for the  $u$ -quark. (b) The NLO  $Q^2$  evolution of  $h_1$  and  $g_1$  for the  $u$ -quark. This figure is taken from Ref. <sup>26</sup>

In Ref. <sup>30</sup>, the Regge asymptotics of  $h_1$  was studied and the small- $x$  behavior was predicted to be  $h_1(x) \sim \text{constant}$  ( $x \rightarrow 0$ ). On the other hand, the rightmost singularity of  $\gamma_n^{h(0)}$  and  $\gamma_n^{h(1)}$  are, respectively, located at  $n = -2$  and  $n = -1$  in the complex  $n$  plane, which, respectively, corresponds to  $h_1(x) \sim x$  and  $h_1(x) \sim \text{constant}$  as  $x \rightarrow 0$ . Therefore inclusion of the NLO effect in the DGLAP asymptotics gives consistent behavior at  $x \rightarrow 0$  as the Regge asymptotics. This is in contrast to the (nonsinglet)  $f_1$  and  $g_1$  distributions, whose LO and NLO DGLAP asymptotics are the same.

One of the interesting applications of the obtained NLO  $Q^2$  evolution of  $h_1$  is the preservation of the Soffer's inequality,<sup>31</sup>  $2|h_1^a(x, Q^2)| \leq f_1^a(x, Q^2) + g_1^a(x, Q^2)$ . Although the validity of this inequality hinges on schemes beyond LO<sup>32</sup>, the NLO  $Q^2$  evolution maintains the inequality at  $Q^2 > Q_0^2$  if it is

satisfied at some (low) scale  $Q_0^2$  in suitably defined factorization schemes such as  $\overline{\text{MS}}$  and Drell-Yan factorization schemes.<sup>33,24</sup>

As was discussed in Sec. 2, a physical cross section is a convolution of a parton distribution and a short distance cross section. (See (1) and (2)) For the double transverse spin asymmetry ( $A_{TT}$ ) in the Drell-Yan process, the NLO short distance cross section has been calculated in Ref.<sup>34</sup> in the  $\overline{\text{MS}}$  scheme. The analysis on  $A_{TT}$  combined with the NLO transversity distribution predicts modest but not negligible NLO effect.<sup>35</sup>

### 2.3 $Q^2$ -evolution of $h_L(x, Q^2)$ and its $N_c \rightarrow \infty$ limit

In general, higher twist ( $\tau \geq 3$ ) distributions represent quark-gluon correlation in the nucleon. Using the QCD equation of motion (see (33) later), one obtains from (4) the following relation ( $m_q = 0$ )<sup>36</sup>:

$$h_L(x, \mu^2) = 2x \int_x^1 \frac{dy}{y^2} h_1(y, \mu^2) + \tilde{h}_L(x, \mu^2), \quad (11)$$

$$\begin{aligned} \tilde{h}_L(x, \mu^2) &= \frac{iP^+}{M} \int_{-\infty}^{\infty} \frac{dz^-}{2\pi} e^{-2ixP \cdot z} \int_0^1 u du \int_{-u}^u t dt \\ &\times \langle PS_{\parallel} | \bar{\psi}(uz) i\gamma_5 \sigma_{\mu\alpha} g G_{\nu}^{\alpha}(tz) z^{\mu} z^{\nu} \psi(-uz) | PS_{\parallel} \rangle, \end{aligned} \quad (12)$$

where  $z^2 = 0$ ,  $z^+ = 0$  and  $S_{\parallel}$  stands for the longitudinal polarization for the nucleon ( $S^{\mu} = S_{\parallel}^{\mu} = p^{\mu} - \frac{M^2}{2} n^{\mu}$ ). This equation means that  $h_L$  consists of the twist-2 contribution and  $\tilde{h}_L$  which represents quark-gluon correlation in the nucleon. We call the latter contribution ‘‘purely twist-3’’ contribution. (Expansion of (12) produces twist-3 local operators. See (15) below.) Equation (11) reminds us of the Wandzura-Wilczek relation<sup>37</sup> for  $g_T$ :

$$g_T(x, \mu^2) = \int_x^1 \frac{dy}{y} g_1(y, \mu^2) + \tilde{g}_T(x, \mu^2). \quad (13)$$

For  $e$  and  $\tilde{g}_T$ , one can write down relations similar to (12).

The  $Q^2$ -evolution of the first and second terms in (11) is described separately. The evolution of  $\tilde{h}_L$  is quite complicated. A detailed analysis of (12) leads to the following relation for the  $n$ -th moment of  $\tilde{h}_L$ <sup>4</sup>:

$$\mathcal{M}_n[\tilde{h}_L(\mu^2)] = \sum_{k=2}^{[(n+1)/2]} \left(1 - \frac{2k}{n+2}\right) \frac{1}{2M} \langle PS_{\parallel} | R_{nk}(\mu) | PS_{\parallel} \rangle, \quad (14)$$

$$R_{nk} = \frac{1}{2} [\bar{\psi} \sigma^{\lambda\alpha} n_{\lambda} i\gamma_5 (in \cdot D)^{k-2} i g G_{\nu\alpha} n^{\nu} (in \cdot D)^{n-k} \psi - (k \rightarrow n - k + 2)]. \quad (15)$$

We note that the number of independent operators  $\{R_{nk}\}$  ( $k = 2, \dots, [(n+1)/2]$ ) increases with  $n$ . In the  $Q^2$ -evolution, the mixing among  $\{R_{nk}\}$  occurs and the renormalization is described by the anomalous dimension matrix  $[\gamma_n(g)]_{kl}$  for  $\{R_{nk}\}$ . If we put the LO anomalous dimension matrix for  $\{R_{nk}\}$  as  $[\gamma_n(g)]_{kl} = (\alpha_s/2\pi)[X_n]_{kl}$  corresponding to (9), the solution to the renormalization group equation for  $\{R_{nk}\}$  takes the following matrix form:

$$\langle PS_{\parallel} | R_{nk}(Q^2) | PS_{\parallel} \rangle = \sum_{l=2}^{[(n+1)/2]} \left[ L^{X_n/\beta_0} \right]_{kl} \langle PS_{\parallel} | R_{nl}(\mu^2) | PS_{\parallel} \rangle, \quad (16)$$

where  $L \equiv \frac{\alpha_s(Q^2)}{\alpha_s(\mu^2)}$ .  $X_n$  for  $\tilde{h}_L$  was derived in Ref.<sup>38</sup>. The  $Q^2$ -evolution for  $\tilde{g}_T$  and  $e$  is also described by matrix equation similar to (16), and the solution was obtained in Refs.<sup>39,40</sup> for  $g_T$  and in Ref.<sup>41</sup>

for  $e$ .<sup>42</sup> As is clear from (14) and (16)  $\mathcal{M}_n[\tilde{h}_L(Q^2)]$  and  $\mathcal{M}_n[\tilde{h}_L(\mu^2)]$  are not connected by a simple equation as in the case for the twist-2 distribution (see (7)).<sup>43</sup> Although (16) gives complete prediction for the  $Q^2$  evolution, it is generally difficult to distinguish contribution from many operators in the analysis of experiments.

In order to get a rough idea on the  $Q^2$ -evolution of  $\tilde{h}_L$ , we plotted the eigenvalues of  $X_n$  in Fig. 4 (right). For comparison, we also showed in the same figure the LO anomalous dimension  $\gamma_n^{(0)}/2$  for  $h_1$ . (Note the difference in convention between (7) and (16).) As is clear from this figure, the  $Q^2$  evolution of  $\tilde{h}_L$  is much faster than that of  $h_1$ . (See discussion below.)

It has been shown in Refs.<sup>44,36,41</sup> that at large  $N_c$  (the number of colors), a great simplification occurs in the  $Q^2$ -evolution of the twist-3 distributions. Recall  $X_n$  in (16) is a function of two Casimir operators  $C_G = N_c$  and  $C_F = \frac{N_c^2-1}{2N_c}$ . If one takes  $N_c \rightarrow \infty$ , i.e.  $C_F \rightarrow N_c/2$ , (14) and (16) is reduced to

$$\mathcal{M}_n[\tilde{h}_L(Q^2)] = L^{\tilde{\gamma}_n^h/\beta_0} \mathcal{M}_n[\tilde{h}_L(\mu^2)], \quad (17)$$

$$\tilde{\gamma}_n^h = 2N_c \left( \sum_{j=1}^n \frac{1}{j} - \frac{1}{4} + \frac{3}{2(n+1)} \right). \quad (18)$$

This evolution equation is just like those for the twist-2 distributions (see (7)). In Fig. 4 (left), we showed the distribution of the eigenvalues of  $X_n$  obtained numerically at  $N_c \rightarrow \infty$ . The solid line is the analytic solution in (18), which shows (18) corresponds to the lowest eigenvalues at  $N_c \rightarrow \infty$ . Since (17) was obtained by a mere replacement  $C_F \rightarrow N_c/2$  in (16), the correction to the result is of  $O(1/N_c^2) \sim 10\%$  level, which gives enough accuracy for practical applications.

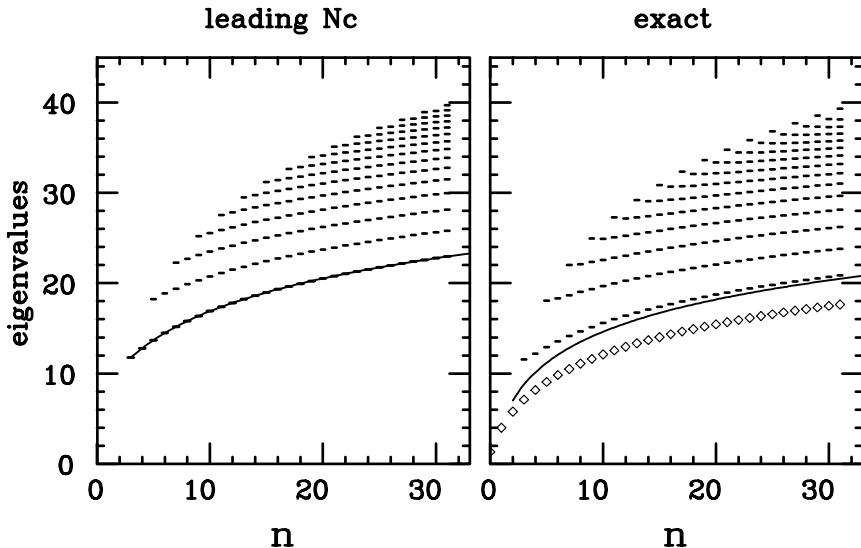


Figure 4: (Right) Complete spectrum of the eigenvalues of the anomalous dimension matrix for  $\tilde{h}_L$  obtained in Ref. <sup>38</sup>. The symbol  $\diamond$  denotes the one-loop anomalous dimension for  $h_1$ . The solid line is the anomalous dimension (21) at large  $n$ . (Left) Spectrum of the eigenvalues of the anomalous dimension matrix for  $\tilde{h}_L$  at large  $N_c$ . The solid line denotes the analytic solution given in (18). This figure is taken from Ref. <sup>36</sup>.

This large- $N_c$  simplification is a consequence of the fact that the coefficients of  $R_{nk}$  in (14) constitutes the *left* eigenvector of  $X_n$  corresponding to the eigenvalue  $\tilde{\gamma}_n^h$  in this limit:

$$\sum_{k=2}^{[(n+1)/2]} \left( 1 - \frac{2k}{n+2} \right) [X_n]_{kl} = - \left( 1 - \frac{2l}{n+2} \right) \tilde{\gamma}_n^h, \quad (19)$$

which implies that all the *right* eigenvectors of  $X_n$  except the one corresponding to  $\tilde{\gamma}_n^h$  are orthogonal to the vector consisting of  $\left(1 - \frac{2k}{n+2}\right)$ . This leads to (17).

This large- $N_c$  simplification of the  $Q^2$  evolution was proved for the nonsinglet  $\tilde{g}_T$  in Ref.<sup>44</sup> and for  $\tilde{h}_L$  and  $e$  in Ref.<sup>36</sup>. The corresponding anomalous dimensions for  $\tilde{g}_T$  and  $e$  are, respectively,

$$\begin{aligned}\tilde{\gamma}_n^g &= 2N_c \left( \sum_{j=1}^n \frac{1}{j} - \frac{1}{4} + \frac{1}{2(n+1)} \right), \\ \tilde{\gamma}_n^e &= 2N_c \left( \sum_{j=1}^n \frac{1}{j} - \frac{1}{4} - \frac{1}{2(n+1)} \right).\end{aligned}\quad (20)$$

Corresponding to three twist-3 distributions in table 1, there are three independent twist-3 fragmentation functions.<sup>9</sup> (Their number is doubled to 6 if one includes final state interactions. See Ref.<sup>9</sup>) It has been shown in Ref.<sup>45</sup> that at large  $N_c$  the  $Q^2$  evolution of all these nonsinglet fragmentation functions is also described by a simple evolution equation similar to (17). Therefore the simplification of the twist-3 evolution equation is universal to all twist-3 nonsinglet distribution and fragmentation functions.

To illustrate the actual  $Q^2$  evolution of  $h_L$ , we have applied (17) to the bag model calculation of  $h_L$ .<sup>46</sup> (Fig. 5) Fig. 5(a) shows the bag calculation of  $h_L$ . At the bag scale, purely twist-3 contribution  $\tilde{h}_L$  is comparable to the twist-2 contribution. After the  $Q^2$  evolution to  $Q^2 = 10 \text{ GeV}^2$ ,  $h_L$  is dominated by the twist-2 contribution (Fig. 5(b)). This can be ascribed to two facts: One is the large anomalous dimension (18) compared with the LO anomalous dimension of  $h_1$  ( $\diamond$  in the right figure of Fig. 4). The other is the presence of a node for  $\tilde{h}_L(x, Q^2)$ , which is taken as model independent due to the constraint  $\int_0^1 dx \tilde{h}_L(x, Q^2) = 0$ ,<sup>47</sup> which is an analogue of the Burkhardt-Cottingham sum rule for  $g_2(x, Q^2)$ .<sup>48</sup> A similar calculation was done for  $g_T$  in Ref.<sup>49</sup>. Using these model calculations, the longitudinal-transverse spin asymmetry,  $A_{LT}$ , for the polarized Drell-Yan process was estimated in Ref.<sup>50</sup>.

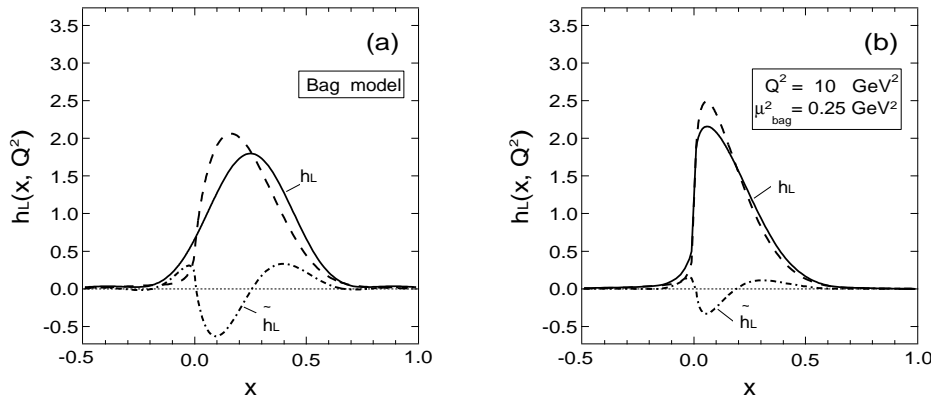


Figure 5: (a) Bag model prediction for  $h_L$ . The dashed line represents the twist-2 contribution to  $h_L$ . (b) Bag model prediction for  $h_L$  evolved to  $Q^2 = 10 \text{ GeV}^2$  assuming the bag scale is  $\mu_{\text{bag}}^2 = 0.25 \text{ GeV}^2$ . These figures are taken from Ref.<sup>46</sup>

Another simplification of the twist-3 evolution occurs at  $n \rightarrow \infty$ .<sup>44,36</sup> In this limit, all the twist-3 distributions obey a simple DGLAP equation (17) with a common anomalous dimension which is

slightly shifted from (18) and (20):

$$\gamma_n = 4C_F \left( \sum_{j=1}^n \frac{1}{j} - \frac{3}{4} \right) + N_c. \quad (21)$$

This evolution equation satisfies the complete evolution equation to the  $O(\ln(n)/n)$  accuracy<sup>44</sup>. In the right figure of Fig. 4, (21) is shown by the solid line. One sees that it is close to the lowest eigenvalues except for small  $n$ . Combined with this  $n \rightarrow \infty$  result, the large- $N_c$  evolution equation in (17) with (18) and (20) for each distribution is valid to  $O((1/N_c^2)\ln(n)/n)$  accuracy.

### 3 Light-cone Distribution Amplitudes of Vector Mesons in QCD

In this section we present a systematic analysis on the light-cone distribution amplitudes (wave functions)<sup>51</sup> of the vector mesons ( $\rho$ ,  $\omega$ ,  $\phi$ ,  $K^*$  etc) following our recent work<sup>53</sup>. These amplitudes are relevant for the preasymptotic correction to various exclusive processes producing vector mesons in the final states, such as  $B$  meson decay,  $B \rightarrow \ell\nu V$  (semi-leptonic),  $B \rightarrow \gamma V$  (radiative), and the electroproduction,  $\gamma^* + N \rightarrow N' + V$ , etc. In particular, we show that the classification and analysis of the light-cone distribution amplitudes for vector mesons can be done in parallel with that of the distribution functions of the nucleon. (Analysis on the light-cone distribution amplitudes for pseudo-scalar mesons is simpler. See e.g. Refs.<sup>51,52</sup>.) For definiteness, we discuss the  $\rho^-$  meson wave functions. Extension to other vector mesons is straightforward.

#### 3.1 Definition and Classification

For the  $\rho^-$ -meson moving in the positive  $+\hat{e}_3$  direction, the light-cone wave functions are defined as

$$\phi(u, \mu^2) = P^+ \int_{-\infty}^{\infty} \frac{dz^-}{2\pi} e^{iuP \cdot z} \langle 0 | \bar{u}(0) \Gamma d(z) |_{\mu} | \rho^-(P, \lambda) \rangle, \quad (22)$$

where  $|\rho^-(P\lambda)\rangle$  stands for the  $\rho^-$ -meson (mass  $m_\rho$ ) state with the momentum  $P$  and the polarization vector  $e_\mu^{(\lambda)}$ ;  $P^2 = m_\rho^2$ ,  $e^{(\lambda)2} = -1$ ,  $P \cdot e^{(\lambda)} = 0$ .  $\Gamma$  denotes generic  $\gamma$  matrices and  $z^-$  is the only nonzero component of the space time coordinate  $z$ . The variable  $u$  in  $\phi(u)$  represents a fraction of “+”-momentum  $P^+$  carried by  $d$  quark and  $\phi$  has a support on  $0 < u < 1$ . Here and below the gauge link operator  $[0, z] \equiv P \exp\{ig \int_1^0 dt z^\mu A_\mu(tz)\}$  which restores gauge invariance is suppressed for simplicity. The only difference between the wave function (22) and the distribution functions (3) is that the latter is a forward matrix elements while the former is a vacuum-to-meson transition amplitude. In order to classify the wave functions (22), it is convenient to introduce two light-like vectors  $p$  and  $n$  as was done in section 2.1 in (4). They satisfy the relations  $p \cdot n = 1$ ,  $P_\mu = p_\mu + \frac{1}{2} m_\rho^2 n_\mu$  and  $e_\mu^{(\lambda)} = (e^{(\lambda)} \cdot n) p_\mu + (e^{(\lambda)} \cdot p) n_\mu + e_{\perp\mu}^{(\lambda)}$ . We introduce two coupling constants  $f_\rho$  and  $f_\rho^T$  by the relation

$$\langle 0 | \bar{u}(0) \gamma_\mu d(0) | \rho^-(P\lambda) \rangle = f_\rho m_\rho e_\mu^{(\lambda)}, \quad (23)$$

and

$$\langle 0 | \bar{u}(0) \sigma_{\mu\nu} d(0) | \rho^-(P\lambda) \rangle = f_\rho^T \left( e_\mu^{(\lambda)} P_\nu - e_\nu^{(\lambda)} P_\mu \right). \quad (24)$$

With these definitions the classification of (22) can be done based on spin, chirality and twist, as was the case for the distribution functions in the nucleon. The only difference is (i)  $e_\mu^{(\lambda)}$  is a vector, while  $S_\mu$  for the nucleon is an axial vector, and (ii) the wave function (22) should be linear in  $e_\mu^{(\lambda)}$ , since it is a matrix element between the vacuum and the  $\rho$  meson state.

Twist	2	3	4
	$O(1)$	$O(1/Q)$	$O(1/Q^2)$
$e_{\parallel}$	$\phi_{\parallel}$	$h_{\parallel}^{(t)}, h_{\parallel}^{(s)}$	$g_3$
$e_{\perp}$	$\underline{\phi_{\perp}}$	$g_{\perp}^{(v)}, g_{\perp}^{(a)}$	$\underline{h_3}$

Table 2: Spin, twist and chiral classification of the  $\rho$  meson distribution amplitudes. Underlined ones are chiral-odd.

The explicit definitions of the chiral-odd  $\rho$  distribution amplitudes are:

$$\begin{aligned}
& \int \frac{d\eta}{2\pi} e^{i\eta u} \langle 0 | \bar{u}(0) \sigma_{\mu\nu} d(\eta n) |_{\mu} \rho^{-}(P, \lambda) \rangle \\
&= i f_{\rho}^T \left[ (e_{\perp\mu}^{(\lambda)} p_{\nu} - e_{\perp\nu}^{(\lambda)} p_{\mu}) \phi_{\perp}(u, \mu^2) + (p_{\mu} n_{\nu} - p_{\nu} n_{\mu}) (e^{(\lambda)} \cdot n) m_{\rho}^2 h_{\parallel}^{(t)}(u, \mu^2) \right. \\
&\quad \left. + \frac{1}{2} (e_{\perp\mu}^{(\lambda)} n_{\nu} - e_{\perp\nu}^{(\lambda)} n_{\mu}) m_{\rho}^2 h_3(u, \mu^2) \right], \tag{25}
\end{aligned}$$

and

$$\int \frac{d\eta}{2\pi} e^{i\eta u} \langle 0 | \bar{u}(0) d(\eta n) |_{\mu} \rho^{-}(P, \lambda) \rangle = \frac{1}{2} \left( f_{\rho}^T - f_{\rho} \frac{m_u + m_d}{m_{\rho}} \right) (e^{(\lambda)} \cdot n) m_{\rho}^2 \frac{dh_{\parallel}^{(s)}(u, \mu^2)}{du}, \tag{26}$$

and the chiral-even distribution amplitudes are defined as

$$\begin{aligned}
& \int \frac{d\eta}{2\pi} e^{i\eta u} \langle 0 | \bar{u}(0) \gamma_{\mu} d(\eta n) |_{\mu} \rho^{-}(P, \lambda) \rangle \\
&= f_{\rho} m_{\rho} \left[ p_{\mu} (e^{(\lambda)} \cdot n) \phi_{\parallel}(u, \mu^2) + e_{\perp\mu}^{(\lambda)} g_{\perp}^{(v)}(u, \mu^2) - \frac{1}{2} n_{\mu} (e^{(\lambda)} \cdot n) m_{\rho}^2 g_3(u, \mu^2) \right] \tag{27}
\end{aligned}$$

and

$$\int \frac{d\eta}{2\pi} e^{i\eta u} \langle 0 | \bar{u}(0) \gamma_{\mu} \gamma_5 d(\eta n) |_{\mu} \rho^{-}(P, \lambda) \rangle = \frac{i}{4} \left( f_{\rho} - f_{\rho}^T \frac{m_u + m_d}{m_{\rho}} \right) m_{\rho} \epsilon_{\mu}^{\nu\alpha\beta} e_{\perp\nu}^{(\lambda)} p_{\alpha} n_{\beta} \frac{dg_{\perp}^{(a)}(u, \mu^2)}{du} \tag{28}$$

All the distribution amplitudes  $\phi = \{\phi_{\parallel}, \phi_{\perp}, h_{\parallel}^{(s)}, h_{\parallel}^{(t)}, g_{\perp}^{(v)}, g_{\perp}^{(a)}, h_3, g_3\}$  are normalized as  $\int_0^1 du \phi(u) = 1$ .

The appearance of the derivative form for  $h_{\parallel}^{(s)}$  and  $g_{\perp}^{(a)}$  in (26) and (28) is consistent with the relation  $\langle 0 | \bar{u}(0) \Gamma d(0) |_{\mu} \rho^{-}(P, \lambda) \rangle = 0$  for  $\Gamma = 1, \gamma_{\mu} \gamma_5$ . The various factors in front of  $\phi(u)$  in (25)-(28) can be derived by the normalization condition for  $\phi$  and the QCD equation of motion. Dimensional analysis of (25)-(28) determines the twist of each wave function, following the same argument in section 2.1. Table 2 summarizes the classification of  $\phi$ 's. If one ignore the mass difference between the  $u$  and  $d$  quarks, the G-parity invariance leads to  $\phi(u) = \phi(1-u)$ .

Similarly to the case of the twist-3 distribution functions (see (11) and (12)), the twist-3 wave functions  $h_{\parallel}^{(s)}, h_{\parallel}^{(t)}, g_{\perp}^{(v)}$  and  $g_{\perp}^{(a)}$  contain the higher Fock component describing the multi-particle component in the wave function. In order to reveal this, we define three-particle twist-3 quark-antiquark-gluon distribution amplitudes as

$$\int \frac{d\eta}{2\pi} \int \frac{d\zeta}{2\pi} e^{i\eta\alpha_d} e^{i\zeta\alpha_u} \langle 0 | \bar{u}(\zeta n) \gamma_{\alpha} g G_{\mu\nu}(0) d(\eta n) |_{\mu} \rho^{-}(P, \lambda) \rangle = i p_{\alpha} [p_{\mu} e_{\perp\nu}^{(\lambda)} - p_{\nu} e_{\perp\mu}^{(\lambda)}] f_{3\rho}^V \mathcal{V}(\alpha_d, \alpha_u) + \dots \tag{29}$$

$$\int \frac{d\eta}{2\pi} \int \frac{d\zeta}{2\pi} e^{i\eta\alpha_d} e^{i\zeta\alpha_u} \langle 0 | \bar{u}(\zeta n) \gamma_{\alpha} \gamma_5 g \tilde{G}_{\mu\nu}(0) d(\eta n) |_{\mu} \rho^{-}(P, \lambda) \rangle = p_{\alpha} [p_{\nu} e_{\perp\mu}^{(\lambda)} - p_{\mu} e_{\perp\nu}^{(\lambda)}] f_{3\rho}^A \mathcal{A}(\alpha_d, \alpha_u) + \dots \tag{30}$$

$$\begin{aligned}
& \int \frac{d\eta}{2\pi} \int \frac{d\zeta}{2\pi} e^{i\eta\alpha_d} e^{i\zeta\alpha_u} \langle 0 | \bar{u}(\zeta n) \sigma_{\alpha\beta} g G_{\mu\nu}(0) d(\eta n) |_{\mu} \rho^{-}(P, \lambda) \rangle = \\
&= \frac{1}{2} (e^{(\lambda)} \cdot n) [p_{\alpha} p_{\mu} g_{\beta\nu}^{\perp} - p_{\beta} p_{\mu} g_{\alpha\nu}^{\perp} - p_{\alpha} p_{\nu} g_{\beta\mu}^{\perp} + p_{\beta} p_{\nu} g_{\alpha\mu}^{\perp}] f_{3\rho}^T m_{\rho} \mathcal{T}(\alpha_d, \alpha_u) + \dots, \tag{31}
\end{aligned}$$

where  $g_{\mu\nu}^{\perp} = g_{\mu\nu} - p_{\mu}n_{\nu} - p_{\nu}n_{\mu}$ , the ellipses stand for Lorentz structures of twist higher than three<sup>56</sup>, and  $\mathcal{V}, \mathcal{A}, \mathcal{T}$  refers in an obvious way to the vector, axial-vector and tensor distributions.  $\alpha_d, \alpha_u$  and  $1 - \alpha_d - \alpha_u$  are the momentum fractions of  $d$  quark,  $u$  quark and gluon, respectively, and  $\mathcal{V}, \mathcal{A}, \mathcal{T}$  have a support on  $\alpha_{u,d} > 0, \alpha_u + \alpha_d < 1$ . When the quark masses are the same, the G-parity invariance implies that the function  $\mathcal{A}$  is symmetric and the functions  $\mathcal{V}$  and  $\mathcal{T}$  are antisymmetric under the interchange  $\alpha_u \leftrightarrow \alpha_d$ . This motivates us to define the coupling constants  $f_{3\rho}^V, f_{3\rho}^A, f_{3\rho}^T$  by the normalization conditions for  $\{\mathcal{V}, \mathcal{A}, \mathcal{T}\}$ :

$$\begin{aligned} \int_0^1 d\alpha_d \int_0^{1-\alpha_d} d\alpha_u (\alpha_d - \alpha_u) \mathcal{V}(\alpha_d, \alpha_u) &= 1, \\ \int_0^1 d\alpha_d \int_0^{1-\alpha_d} d\alpha_u \mathcal{A}(\alpha_d, \alpha_u) &= 1, \\ \int_0^1 d\alpha_d \int_0^{1-\alpha_d} d\alpha_u (\alpha_d - \alpha_u) \mathcal{T}(\alpha_d, \alpha_u) &= 1. \end{aligned} \quad (32)$$

Distribution amplitudes defined in this section contain only the light-cone momentum fraction. One might ask what about the intrinsic transverse momentum of quarks which causes power correction to an exclusive process. Are they missing in this formalism? The answer is no. One can show that in calculating the amplitude for an exclusive process the effect of intrinsic transverse momentum of quarks is systematically and Gauge invariantly incorporated by considering the multi-particle (three or more) distribution amplitudes, i.e., it can be reexpressed in the form of higher twist distribution amplitudes.

### 3.2 QCD Equation of Motion

The two- and three-particle distribution amplitudes introduced in the previous subsection are not independent among one another, but are constrained by the QCD equation of motion. This can be most conveniently done by using the identities among the nonlocal operators defining each amplitude: For example, relevant identities for the chiral-odd distribution amplitudes are

$$\begin{aligned} \frac{\partial}{\partial x_{\mu}} \{ \bar{u}(x) \sigma_{\mu\nu} x^{\nu} d(-x) \} &= \\ &= i \int_{-1}^1 dv v \bar{u}(x) x^{\alpha} \sigma_{\alpha\beta} x^{\mu} g G_{\mu\beta}(vx) d(-x) \\ &\quad - i x^{\beta} \partial_{\beta} \{ \bar{u}(x) d(-x) \} - (m_u - m_d) \bar{u}(x) \not{x} d(-x), \end{aligned} \quad (33)$$

$$\begin{aligned} \bar{u}(x) d(-x) - \bar{u}(0) d(0) &= \\ &= \int_0^1 dt \int_{-t}^t dv \bar{u}(tx) x^{\alpha} \sigma_{\alpha\beta} x^{\mu} g G_{\mu\beta}(vx) d(-tx) \\ &\quad + i \int_0^1 dt \partial^{\alpha} \{ \bar{u}(tx) \sigma_{\alpha\beta} x^{\beta} d(-tx) \} \\ &\quad + i(m_u + m_d) \int_0^1 dt \bar{u}(tx) \not{x} d(-tx). \end{aligned} \quad (34)$$

Here we introduced a shorthand notation for the derivative over the total translation:

$$\partial_{\alpha} \{ \bar{u}(tx) \Gamma[tx, -tx] d(-tx) \} \equiv \frac{\partial}{\partial y^{\alpha}} \{ \bar{u}(tx+y) \Gamma[tx+y, -tx+y] d(-tx+y) \} \Big|_{y \rightarrow 0}, \quad (35)$$

with the generic Dirac matrix structure  $\Gamma$ . Sandwiching these identities by the vacuum and the  $\rho$  meson state, we obtain the relation among two- and three- particle distribution amplitudes. We

finally obtain for the chiral-odd distribution amplitudes as

$$(1 - \delta_+) h_{\parallel}^{(s)}(u) = \bar{u} \int_0^u dv \frac{1}{v} \Phi(v) + u \int_u^1 dv \frac{1}{v} \Phi(v), \quad (36)$$

and

$$\begin{aligned} h_{\parallel}^{(t)}(u) &= \frac{1}{2} \xi \left( \int_0^u dv \frac{1}{v} \Phi(v) - \int_u^1 dv \frac{1}{v} \Phi(v) \right) + \delta_+ \phi_{\parallel}(u) \\ &+ \zeta_{3\rho}^T \frac{d}{du} \int_0^u d\alpha_d \int_0^{\bar{u}} d\alpha_u \frac{1}{1 - \alpha_u - \alpha_d} \mathcal{T}(\alpha_d, \alpha_u), \end{aligned} \quad (37)$$

where

$$\begin{aligned} \Phi(u) &= 2\phi_{\perp}(u) - \delta_+ \left( \phi_{\parallel}(u) - \frac{1}{2} \xi \phi'_{\parallel}(u) \right) + \frac{1}{2} \delta_- \phi'_{\parallel}(u) \\ &+ \zeta_{3\rho}^T \frac{d}{du} \int_0^u d\alpha_d \int_0^{\bar{u}} d\alpha_u \frac{1}{1 - \alpha_u - \alpha_d} \left( \alpha_d \frac{d}{d\alpha_d} + \alpha_u \frac{d}{d\alpha_u} - 1 \right) \mathcal{T}(\alpha_d, \alpha_u) \end{aligned} \quad (38)$$

with

$$\delta_{\pm} = \frac{f_{\rho}}{f_{\rho}^T} \frac{m_u \pm m_d}{m_{\rho}}, \quad \zeta_{3\rho}^T = \frac{f_{3\rho}^T}{f_{\rho}^T m_{\rho}}. \quad (39)$$

Here and below we use the shorthand notation  $\bar{u} = 1 - u$  and  $\xi = u - (1 - u) = 2u - 1$ . According to the various ‘‘source’’ terms on the right-hand side of (36) and (37), one can decompose the solution in an obvious way into three pieces as

$$\begin{aligned} h_{\parallel}^{(t)}(u) &= h_{\parallel}^{(t)WW}(u) + h_{\parallel}^{(t)g}(u) + h_{\parallel}^{(t)m}(u), \\ h_{\parallel}^{(s)}(u) &= h_{\parallel}^{(s)WW}(u) + h_{\parallel}^{(s)g}(u) + h_{\parallel}^{(s)m}(u), \end{aligned} \quad (40)$$

where  $h_{\parallel}^{(t)WW}(u)$  and  $h_{\parallel}^{(s)WW}(u)$  denote the ‘‘Wandzura-Wilczek’’ type contributions of twist 2 operators,  $h_{\parallel}^{(t)g}(u)$  and  $h_{\parallel}^{(s)g}(u)$  stand for contributions of three-particle distribution amplitudes and  $h_{\parallel}^{(t)m}(u)$  and  $h_{\parallel}^{(s)m}(u)$  are due to the quark mass corrections. This decomposition can be compared with the relation (11) for the twist-3 distribution. In particular, we get

$$\begin{aligned} h_{\parallel}^{(t)WW}(u) &= \xi \left( \int_0^u dv \frac{\phi_{\perp}(v)}{v} - \int_u^1 dv \frac{\phi_{\perp}(v)}{v} \right), \\ h_{\parallel}^{(s)WW}(u) &= 2 \left( \bar{u} \int_0^u dv \frac{\phi_{\perp}(v)}{v} + u \int_u^1 dv \frac{\phi_{\perp}(v)}{v} \right). \end{aligned} \quad (41)$$

Similarly we obtain for the chiral-even distribution amplitudes as

$$(1 - \tilde{\delta}_+) g_{\perp}^{(a)}(u) = \bar{u} \int_0^u dv \frac{1}{v} \Psi(v) + u \int_u^1 dv \frac{1}{v} \Psi(v), \quad (42)$$

and

$$\begin{aligned}
g_{\perp}^{(v)}(u) &= \frac{1}{4} \left[ \int_0^u dv \frac{1}{v} \Psi(v) + \int_u^1 dv \frac{1}{v} \Psi(v) \right] + \tilde{\delta}_+ \phi_{\perp}(u) \\
&+ \zeta_{3\rho}^A \int_0^u d\alpha_d \int_0^{\bar{u}} d\alpha_u \frac{1}{1 - \alpha_d - \alpha_u} \left( \frac{d}{d\alpha_d} + \frac{d}{d\alpha_u} \right) \mathcal{A}(\alpha_d, \alpha_u) \\
&+ \zeta_{3\rho}^V \frac{d}{du} \int_0^u d\alpha_d \int_0^{\bar{u}} d\alpha_u \frac{\mathcal{V}(\alpha_d, \alpha_u)}{1 - \alpha_d - \alpha_u},
\end{aligned} \tag{43}$$

where

$$\begin{aligned}
\Psi(u) &= 2\phi_{\parallel}(u) + \tilde{\delta}_+ \xi \phi'_{\perp}(u) + \tilde{\delta}_- \phi'_{\perp}(u) \\
&+ 2\zeta_{3\rho}^V \frac{d}{du} \int_0^u d\alpha_d \int_0^{\bar{u}} d\alpha_u \frac{1}{1 - \alpha_d - \alpha_u} \left( \alpha_d \frac{d}{d\alpha_d} + \alpha_u \frac{d}{d\alpha_u} \right) \mathcal{V}(\alpha_d, \alpha_u) \\
&+ 2\zeta_{3\rho}^A \frac{d}{du} \int_0^u d\alpha_d \int_0^{\bar{u}} d\alpha_u \frac{1}{1 - \alpha_d - \alpha_u} \left( \alpha_d \frac{d}{d\alpha_d} - \alpha_u \frac{d}{d\alpha_u} \right) \mathcal{A}(\alpha_d, \alpha_u),
\end{aligned} \tag{44}$$

with

$$\tilde{\delta}_{\pm} \equiv \frac{f_{\rho}^{T^2}}{f_{\rho}^2} \delta_{\pm} = \frac{f_{\rho}^T}{f_{\rho}} \frac{m_u \pm m_d}{m_{\rho}}, \quad \zeta_{3\rho}^{V,A} = \frac{f_{3\rho}^{V,A}}{f_{\rho} m_{\rho}}. \tag{45}$$

Eqs. (42) and (43) again allow the decomposition of  $g_{\perp}^{(v)}(u)$  and  $g_{\perp}^{(a)}(u)$  into several terms according to the source terms:

$$\begin{aligned}
g_{\perp}^{(v)}(u) &= g_{\perp}^{(v)WW}(u) + g_{\perp}^{(v)g}(u) + g_{\perp}^{(v)m}(u), \\
g_{\perp}^{(a)}(u) &= g_{\perp}^{(a)WW}(u) + g_{\perp}^{(a)g}(u) + g_{\perp}^{(a)m}(u),
\end{aligned} \tag{46}$$

where  $g_{\perp}^{(v)WW}(u)$  and  $g_{\perp}^{(a)WW}(u)$  denotes the contribution from the twist 2 distribution amplitudes (Wandzura-Wilczek part),  $g_{\perp}^{(v)g}(u)$  and  $g_{\perp}^{(a)g}(u)$  are the contribution from the three-particle distribution amplitudes  $\mathcal{V}$  and  $\mathcal{A}$ .

The relations (36), (37), (42) and (43) are exact in QCD and form a basis for the renormalization and model buildings for the twist-3 wave functions. Wandzura-Wilczek parts in (40) and (46) do not mix with other sources under renormalization. Renormalization and the model building based on the QCD sum rule approach has been carried out in the framework of the conformal expansion for the distribution amplitudes in Refs.<sup>53,54,55</sup>.

## 4 Summary

In the first part of this talk, I discussed the  $Q^2$  evolution of the chiral-odd spin-dependent parton distributions  $h_1(x, Q^2)$  and  $h_L(x, Q^2)$ . The NLO  $Q^2$  evolution for the transversity distribution  $h_1(x, Q^2)$  was completed in the  $\overline{\text{MS}}$  scheme. This means the  $Q^2$  evolution of all the twist-2 distributions has been understood in the NLO level. The resulting  $Q^2$  evolution of  $h_1(x, Q^2)$  turned out to cause quite different behavior from the helicity distribution  $g_1(x, Q^2)$  in the small  $x$  region. The LO  $Q^2$  evolution for the twist-3 distribution  $h_L(x, Q^2)$  (and  $e(x, Q^2)$ ) was completed. Although their  $Q^2$  evolution is quite complicated due to the mixing among increasing number of quark-gluon-quark operators, it obeys a simple DGLAP equation similar to the twist-2 distribution in the  $N_c \rightarrow \infty$  limit,

as was the case for the  $Q^2$  evolution of the nonsinglet  $g_T(x, Q^2)$  distribution. The same simplification at  $N_c \rightarrow \infty$  was also proved for the twist-3 fragmentation functions. Therefore this large- $N_c$  simplification was proved to be universal for the twist-3 distribution and fragmentation functions.

In the second part of this talk, I presented a systematic analysis on the light-cone distribution amplitudes for the vector mesons relevant for exclusive processes. Classification can be done in parallel with that of the nucleon's parton distribution functions. Constraint relations among two- and three- particle distribution amplitudes are derived using QCD equation of motion. These relations are exact and must be satisfied for model buildings. Renormalization of the two-particle twist-3 distribution amplitudes can also be performed based on these relations.

## Acknowledgements

I would like to thank I.I. Balitsky, P. Ball, V.M. Braun, A. Hayashigaki, Y. Kanazawa, N. Nishiyama and K. Tanaka for the collaboration on the subjects discussed in this talk.

## References

1. See, for example, *Spin Structure of the Nucleon* (World Scientific, 1996, eds. T.-A. Shibata et al.); *SPIN96* (World Scientific, 1997, eds. C.W. de Jager et al.).
2. J.C. Collins, D. Soper and G. Sterman, in *Perturbative Quantum Chromodynamics* (World Scientific, Singapore, 1989, ed. A.H. Mueller), and references quoted therein.
3. J.C. Collins and D.E. Soper, Nucl. Phys. **194**, 445 (1982).
4. R.L. Jaffe and X. Ji, Nucl. Phys. **B375**, 527 (1992).
5. J.P. Ralston and D.E. Soper, Nucl. Phys. **B152**, 109 (1979).
6. X. Artru and M. Mekhfi, Z. Phys. **C45** 669 (1990); Nucl. Phys. **A532** (1991) 351c.
7. J.L. Cortes, B. Pire and J.P. Ralston, Z. Phys. **C55**, 409 (1992).
8. R.L. Jaffe and X. Ji, Phys. Rev. Lett **71**, 2547 (1993).
9. X. Ji, Phys. Rev. **D49**, 114 (1994).
10. R.L. Jaffe, Phys. Rev. **D54**, 6581 (1996).
11. R.L. Jaffe, X. Jin and J. Tang, Phys. Rev. Lett. **80**, 1166 (1998).
12. R.L. Jaffe, Comm. Nucl. Part. Phys. **19**, 239 (1990).
13. The Spin Muon Collaboration (D. Adams et al.), Phys. Lett. **B336**, 125 (1994); E143 Collaboration (K. Abe et al.), Phys. Rev. Lett. **76**, 587 (1996).
14. A.V. Manohar, Phys. Rev. Lett. **65**, 2511 (1990); **66**, 289 (1991); X. Ji, Phys. Lett. **B289**, 137 (1992).
15. P.V. Pobylitsa and M.V. Polyakov, Phys. Lett. **B389**, 350 (1996); V. Barone, T. Calarco and A. Drago, Phys. Lett. **B390**, 287 (1997); L. Gamberg, H. Reinhardt and H. Weigel, Phys. Rev. **D58**, 054014 (1998); M. Wakamatsu and T. Kubota, hep-ph/9809443.
16. For a review on  $h_1$ , see R.L. Jaffe, hep-ph/9710465, in Proc. of 2nd Topical Workshop on Deep Inelastic Scattering off Polarized Targets: Theory Meets Experiment (DESY-Zeuthen, Sep. 1-5, 1997). DESY 97-200, p167.
17. V.N. Gribov and L.N. Lipatov, Sov. J. Nucl. Phys. **15**, 438 (1972), G. A. Altarelli and G. Parisi, Nucl. Phys. **B126**, 298 (1977), Yu. L. Dokshitzer, Sov. Phys. JETP **46**, 641 (1977).
18. E.G. Floratos, D.A. Ross and C.T. Sachrajda, Nucl. Phys. **B129**, 66 (1977); **B139**, 545 (1978) (E); Nucl. Phys. **B152**, 493 (1979).
19. A. Gonzalez-Arroyo, C. Lopez and F.J. Yndurain, Nucl. Phys. **B153**, 161 (1979).
20. G. Curci, W. Furmanski and R. Petronzio, Nucl. Phys. **B175**, 27 (1980), W. Furmanski and R. Petronzio, Phys. Lett **97B**, 437 (1980).
21. R. Mertig, W.L. van Neerven, Z. Phys. **C70** 637 (1996); W. Vogelsang, Phys. Rev. **D54** 2023 (1996); Nucl. Phys. **B475**, 47 (1996).
22. M. Glück, E. Reya and A. Vogt, Z. Phys. **C53**, 127 (1992); A.D. Martin, W.J. Stirling and R.G. Roberts, Phys. Lett. **B354**, 155 (1995); H.L. Lai, et. al. Phys. Rev. **D51**, 4763 (1995).

23. M. Glück, E. Reya, M. Stratmann and W. Vogelsang, Phys. Rev. **D53**, 4775 (1996); T. Gehrmann and W.J. Stirling, Phys. Rev. **D53**, 6100 (1996); G. Altarelli, R. Ball, S. Forte and G. Ridolfi, Nucl. Phys. **B496**, 337 (1997).
24. W. Vogelsang, Phys. Rev. **D57**, 1886 (1998).
25. A. Hayashigaki, Y. Kanazawa and Y. Koike, Phys. Rev. **D56**, 7350 (1997).
26. A. Hayashigaki, Y. Kanazawa and Y. Koike, hep-ph/9710421, in Proc. of 2nd Topical Workshop on Deep Inelastic Scattering off Polarized Targets: Theory Meets Experiment (DESY-Zeuthen, Sep. 1-5, 1997) DESY 97-200, p. 157.
27. V. Barone, T. Calarco and A. Drago, Phys. Rev. **D56**, 527 (1997).
28. S. Scopetta and V. Vento, Phys. Lett. **B424**, 25 (1996).
29. S. Aoki, M. Doui, T. Hatsuda and Y. Kuramashi, Phys. Rev. **D56**, 433 (1997).
30. R. Kirschner, L. Mankiewicz, A. Schäfer and L. Szymanowski, Z. Phys. **C74**, 501 (1997); R. Kirschner, hep-ph/9710253, in Proc. of 2nd Topical Workshop on Deep Inelastic Scattering off Polarized Targets: Theory Meets Experiment (DESY-Zeuthen, 1997) DESY 97-200, p. 259.
31. J. Soffer, Phys. Rev. Lett. **74**, 1292 (1995).
32. G.R. Goldstein, R.L. Jaffe and X. Ji, Phys. Rev. **D52**, 5006 (1995).
33. C. Bourrely, J. Soffer and O.V. Teryaev, Phys. Lett. **B420**, 375 (1998).
34. A.P. Contogouris, B. Kamal and Z. Merebashvili, Phys. Lett. **B337**, 169 (1994); B. Kamal, Phys. Rev. **D53**, 1142 (1996).
35. O. Martin, A. Schäfer, M. Stratmann, and W. Vogelsang, Phys. Rev. **D57**, 3084 (1998).
36. I.I. Balitsky, V.M. Braun, Y. Koike and K. Tanaka, Phys. Rev. Lett. **77**, 3078 (1996).
37. W. Wandzura and F. Wilczek, Phys. Lett. **B72**, 195 (1977).
38. Y. Koike and K. Tanaka, Phys. Rev. **D51**, 6125 (1995).
39. E.V. Shuryak and A.I. Vainshtein, Nucl. Phys. **B201**, 141 (1982); A.P. Bukhvostov, E.A. Kuraev and L.N. Lipatov, Sov. Phys. JETP **60**, 22 (1984). P.G. Ratcliffe, Nucl. Phys. **B264**, 493 (1986); I.I. Balitsky and V.M. Braun, Nucl. Phys. **B311**, 541 (1988/89); X. Ji and C. Chou, Phys. Rev **D42**, 3637 (1990); D. Müller, Phys. Lett. **B407**, 314 (1997).
40. J. Kodaira, Y. Yasui and T. Uematsu, Phys. Lett. **B344**, 348 (1995); J. Kodaira, Y. Yasui, K. Tanaka and T. Uematsu, Phys. Lett. **B387**, 855 (1996); J. Kodaira, T. Nasuno, H. Tochimura, K.Tanaka, Y. Yasui, Prog. Theor. Phys. **99**, 315 (1998).
41. Y. Koike and N. Nishiyama, Phys. Rev. **D55**, 3068 (1997).
42. In carrying out the renormalization of the twist-3 distributions in the covariant gauge, there arises complication due to the mixing with an equation-of-motion (EOM) operator and a BRS exact operator as well as “alien” operators in the intermediate step. For this point and a method to handle the issue, see Refs. <sup>38,40</sup> and a review J. Kodaira and K. Tanaka, hep-ph/9812449 to appear in Prog. Theor. Phys.
43. For the evolution equation for  $h_L$  and  $e$ , see A.V. Belitsky and D. Müller, Nucl. Phys. **B503**, 279 (1997).
44. A. Ali, V.M. Braun and G. Hiller, Phys. Lett. **B266**, 117 (1991); see also K. Sasaki, Phys. Rev. **D58**, 094007 (1998).
45. A.V. Belitsky, Phys. Lett. **B312**, 312 (1997); A.V. Belitsky and E.A. Kuraev, Nucl. Phys. **B499**, 301 (1997).
46. Y. Kanazawa and Y. Koike, Phys. Lett. **B403**, 357 (1997).
47. M. Burkardt, in *Proc. 10th International Symposium on High Energy Spin Physics, Hagoya, Japan, Nov. 1992.* (Ed. by Hasegawa et al., Universal Academy Press, Tokyo, 1993) p35.
48. H. Burkhardt and W.N. Cottingham, Ann. Phys. **56**, 453 (1970).
49. M. Stratmann, Z. Phys. **C60**, 763 (1993).
50. Y. Kanazawa, Y. Koike and N. Nishiyama, Phys. Lett. **B430**, 195 (1998).
51. See, for a review, V.L. Chernyak and A.R. Zhitnisky, Phys. Rep. **112**, 173 (1984).
52. V.M. Braun and I.E. Filyanov, Z. Phys. **C48**, 239 (1990) and the references therein.
53. P. Ball, V.M. Braun, Y. Koike and K.Tanaka, Nucl. Phys. **B529**, 323 (1998).

54. Y. Koike, N. Nishiyama and K. Tanaka, Phys. Lett. **B437**, 153 (1998).
55. K. Tanaka, in these proceedings.
56. For the complete structures, see V.M. Braun and P. Ball, hep-ph/9810475.